



Original article

Fragment-based design, synthesis, and biological evaluation of *N*-substituted-5-(4-isopropylthiophenol)-2-hydroxynicotinamide derivatives as novel Mcl-1 inhibitors

Zhichao Zhang^{a,*}, Chengwu Liu^b, Xiangqian Li^a, Ting Song^{c,d}, Zhiyong Wu^a, Xiaomeng Liang^a, Yan Zhao^c, Xiaoyun Shen^c, Hongbo Chen^{a,*}

^a State Key Laboratory of Fine Chemicals, School of Chemistry, Dalian University of Technology, No.2 Linggong Road, Dalian 116012, PR China

^b Zhejiang Hisun Pharmaceutical Company, Zhejiang 322100, PR China

^c School of Life Science and Technology, Dalian University of Technology, Dalian 116024, PR China

^d State Key Laboratory of Natural and Biomimetic Drugs, Peking University, Beijing 100191, PR China

ARTICLE INFO

Article history:

Received 11 April 2012

Received in revised form

29 October 2012

Accepted 9 December 2012

Available online 17 December 2012

Keywords:

Fragment-based

Apoptosis

Mcl-1

LE

FQ

ABSTRACT

We have previously reported a nanomolar inhibitor of antiapoptotic Mcl-1 protein, 3-thiomorpholin-8-oxo-8H-acenaphtho [1,2-*b*] pyrrole-9-carbonitrile (**S1**). **S1** plays its function by binding to the BH3 groove of Mcl-1. Basing on this spacial structural characteristic, we developed a novel class of Mcl-1 inhibitor using fragment-based drug discovery approach. By dissecting **S1**, we identified the compound **4** with a 2-hydroxypyridine core as the starting fragment. In the following molecular growth, we used the ligand efficiency evaluation and fit quality score to assess the fragments. A novel potent compound, *N*-benzyl-5-(4-isopropylthiophenol)-2-hydroxyl nicotinamide (**12c**), which binds Mcl-1 with an IC₅₀ value of 54 nM was obtained. Compound **12c** demonstrated a better aqueous solubility than **S1**.

© 2012 Elsevier Masson SAS. All rights reserved.

1. Introduction

The Bcl-2 family of proteins plays a key role in the regulation of the critical homeostatic balance between cellular life and death [1–4]. In the antiapoptotic members, Mcl-1 is an important one and it has a critical role separated from that of others in the regulation of apoptosis [5]. As such, in recent years, Mcl-1 has become an attractive target for the treatment of cancer. Due to the small divergence in their BH3 grooves, most of the Bcl-2 inhibitors can not accommodate well inside Mcl-1 [6,7]. We have previously reported a small-molecule 3-thiomorpholin-8-oxo-8H-acenaphtho [1,2-*b*] pyrrole-9-carbonitrile (**S1**) with high affinity toward Mcl-1 protein ($K_i = 58$ nM) [8,9]. However, the poor aqueous solubility of **S1** due to the rigid plane structure would significantly reduce its drugability. Since **S1** holds a new molecular skeleton that different from other BH3 mimetics, it could be dissected into various new fragments.

These fragments could be optimized independently to give chemically distinct Mcl-1 inhibitors as novel antitumor drug candidates. Moreover, the disruption of the planarity and symmetry of the original skeleton could provide better aqueous solubility.

Fragment-based drug discovery (FBDD) is gathering momentum in the pharmaceutical industry because it is more likely to produce a better optimized drug-like compound with lower molecular weight. A number of clinical candidates and advanced leads have been developed via this approach [10–14]. Fragments are compounds of low molecular weight (usually 100–250 Da) and typically have low binding affinities (100–1000 μ M). These fragments can be translated into bigger molecules with nanomolar affinities by using a variety of design strategies, such as fragment optimization, fragment merging or linking, and in situ fragment assembly [15,16]. In theory, ligand efficiency (LE) provides a metric for assessing the quality of the fragments in screening and helps to guide optimization [17,18]. Some retrospective studies found, however, that LE is related intrinsically to molecular size, so it is difficult to compare ligand efficiencies for molecules of disparate sizes. Therefore, a new scaled efficiency metric termed as fit quality (FQ) was proposed to allow for such a comparison. FQ score is an

* Corresponding authors. Tel./fax: +86 411 84986032.

E-mail addresses: zc Zhang@dlut.edu.cn (Z. Zhang), chenhb@dlut.edu.cn (H. Chen).

alternative metric to guide FBDD due to its size-independent judgment [19,20]. Here, we applied fragment-based approaches to get more drug-like Mcl-1 inhibitors based on **S1**. We firstly defragmented **S1** into small pieces to find an ideal starting fragment. Consequently, this fragment was optimized under the guidance of LE and FQ. Ultimately, we got a new potent Mcl-1 inhibitor **12c** with better aqueous solubility than that of **S1**.

2. Chemistry

Compound **5** was prepared according to the method of Hao et al. [21] (Scheme 1). Compounds **6a–b** were prepared according to the method of Powell et al. [22] and Mattay et al. [23]. The syntheses of **6c–d** were accomplished by the reaction of corresponding phenylboronic acid with 5-bromo-2-hydroxynicotinonitrile (**1**) under slightly modified Suzuki-type conditions. Compounds **6e–j** were obtained by reaction of the corresponding thiophenol with **1** in the presence of cesium carbonate. **6k** was synthesized by the reaction of **6g** as reported earlier [24] (Scheme 2).

The target compounds **12a–d** were synthesized according to the route described in Scheme 3, and the starting material 2-chloronicotinic acid (**7**) used in this scheme was prepared from 2-chloronicotinonitrile according to the reported methods [25]. This compound was converted to the acyl chloride with thionyl dichloride under reflux conditions; the acyl chloride was then coupled with different amines to give the acylamide compounds **9a–d** in good yield. Subsequent hydrolysis and bromination of **9a–d** in acetic acid resulted in **11a–d**, and then coupled with 4-isopropylthiophenol in the presence of potassium tert-butoxide and cuprous iodide to produce corresponding compounds **12a–d**.

3. Results and discussion

3.1. Identification of starting point

Our previous investigation has identified that **S1** is an authentic BH3 mimetic as well as a nanomolar inhibitor of Mcl-1 protein [8]. Based on **S1**, we aimed to obtain more Mcl-1 inhibitors with novel scaffolds by using a fragment-based approach. We dissected **S1** into smaller fragment molecules 2-[2-oxo-2H-acenaphthyl-1-ylidene]-malononitrile (**2**), acenaphthenequinone (**3**), and 2-hydroxynicotinonitrile (**4**) (Scheme 4). The binding affinities (K_i) of these fragments were evaluated using fluorescence polarization assays (FPAs) that measure their abilities to competitively displace a Bid-derived peptide from Mcl-1, as described in the biological assay. Affinity alone is neither the first aspect for a drug-likeness, nor the gold standard for monitor fragment-based molecular design. Ligand efficiency (LE) is a common criterion for measuring the quality of a fragment. We then calculated these fragments based on K_i as described [17] (Table 1). In general, an LE of 0.36 kcal mol⁻¹ per heavy atom is required for a 'Rule-of-Three'-compliant fragment (MW ≤300 Da, Clog P ≤3, hydrogen bond donors and acceptors each ≤3), which could ensure a successful

optimization toward the potent leads that still fit 'Rule-of-Five' (MW ≤500 Da, Clog P ≤5, H-bond donors ≤3, H-bond acceptors ≤10) [20]. Although all the four fragments fulfilled the required minimal LE value, the highest LE (LE = 0.60) was found for fragment **4**. Our previous study has found that the carbonyl group of **S1** binds R263 in Mcl-1 through a hydrogen bond [9]. Probably fragment **4** exhibits higher efficiency due to maintaining of this key recognition. Additionally, the smallest size of **4** among these fragments offered it advantages for further drug optimization. The much lower Clog P of **4** (0.665) than that of **2** (1.612) and **3** (2.532) also made it favorable as a drug-like fragment. So, compound **4** was identified as the starting fragment.

3.2. Optimization of starting point

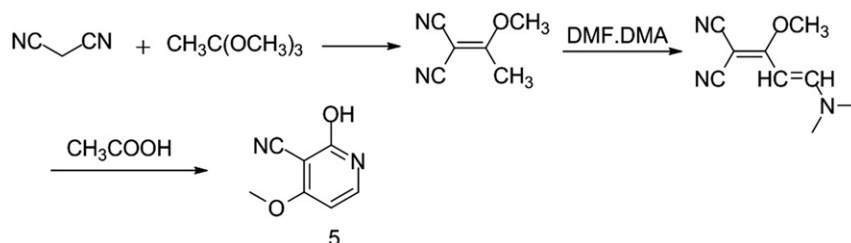
Fragment growth was applied based on **4**. It was noticed that modification of the 6-position of **4** would require a great deal of synthetic labor. A methoxy group was then incorporated at the 4-position, yielding **5** (Scheme 1). Our FPA determined that **5** lost all the binding ability of its initial compound. We then shifted to the 5-position. Firstly, we attached phenyl and naphthyl groups to produce **6a** and **6b** (Scheme 2), respectively. The 10–20 times improved binding affinities suggested that the 5-position is a proper site for further optimization. We consequently synthesized **6c** and **6d** which prolong the substituent at the para position of the phenyl group in **6a**, and **6e–j** which contain corresponding phenyl ring tethered through a sulfur atom linker to the 5-position of **4** (Scheme 2). All the compounds were tested by FPA (Table 1). The competitive binding curves of these compounds to Mcl-1 were outlined in Fig. 1a. LE values of all these optimized compounds were calculated. As shown in Table 1, compounds **6a–j** showed the similar LE with **4** (about 0.4), which made direct comparison problematic. To enable a size-independent comparison of ligands and find a relay molecule for the further fragment growth, we introduced an alternative metric fit quality (FQ) score where each LE value is scaled based on the maximum LE for the heavy atom count of that ligand [19]. The objective is to scale the most efficient ligands so that they have a normalized score of 1.0 regardless of size. FQ score near 1.0 indicates near optimal ligand binding.

According to

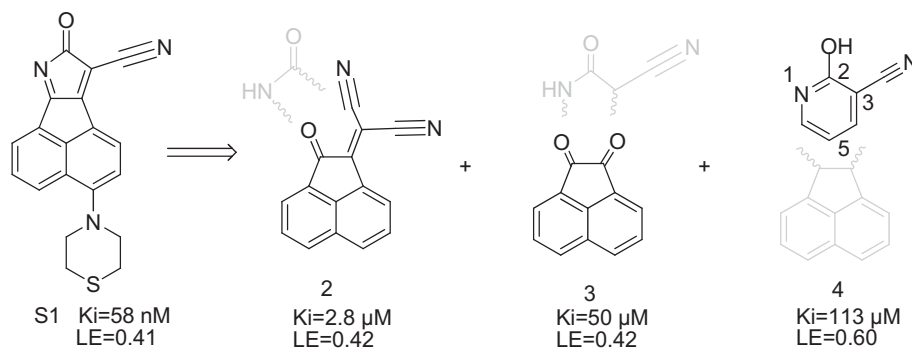
$$FQ = \frac{LE}{LE_{Scale}}$$

$$LE_{Scale} = 0.0715 + \frac{7.5328}{HA} + \frac{25.7079}{HA^2} - \frac{361.4722}{HA^3}$$

where HAC is the heavy atom count [19], we calculated FQ for compounds **4** and **6a–j** (Table 1). When **4** showed 0.82, the FQ declined to about 0.7 for compounds **6a–d**. Compound **6e**, in which a phenyl group was attached to the 5-position of **4** through a sulfur atom linker, showed an increased FQ (0.85). In general, FQ scores should be at least maintained or in most cases even improved



Scheme 1. Synthesis of compound **5**.



Scheme 4. Deconstruction of **S1** into fragments by removing specific groups (highlighted in grey).

improved FQ (0.9) were found for **6g**, whose affinity is 100 times higher than that of **4** (Table 1). But the bigger *t*-amyl (**6h**) at this position showed a steric hindrance that a significant decrease of K_i (7.09 μ M) as well as FQ score (0.75) was found (Table 1). The results suggested that isopropyl (**6g**) provided a proper steric effect at this position. Additionally, replacing the 4-methyl of **6f** with isovolumetric bromine atom (**6i**) or amino group (**6j**) resulted in about 2-fold decrease in affinities. It suggested hydrophilic substituent is unfavorable for affinity at this site.

Next, we chose **6g** as a lead for further structure optimization. Firstly we attached a benzyl group to the 1-position of **6g**, yielding **6k**. The affinity of **6k** showed a significant decrease (15.28 μ M), so did its FQ (0.69) (Table 1). We then shifted to the 3-position of **6g**. We attached hydrophobic groups with increased molecular size to this position to enhance protein interaction because the binding

groove is hydrophobic. To another aspect, replacement of the toxic 3-cyano group could contribute to better drugability. Specifically, we examined isopropyl, *n*-butyl, benzyl and phenylpropyl yielding *N*-isopropyl-5-(4-isopropylthiophenol)-2-hydroxynicotinamide (**12a**), *N*-butyl-5-(4-isopropylthiophenol)-2-hydroxynicotinamide (**12b**), *N*-benzyl-5-(4-isopropylthiophenol)-2-hydroxynicotinamide (**12c**), and *N*-phenylpropyl-5-(4-isopropylthiophenol)-2-hydroxynicotinamide (**12d**), respectively (Scheme 3). Because these compounds interfere with the fluorescence of FAM in FPA, we used an enzyme-linked immunosorbent assay (ELISA) to test their affinities toward Mcl-1 protein (Fig. 1b). Compound **6g** was also tested for comparison (Table 2). Result showed both alkyl and aryl substituent were well accepted showing enhanced potency relative to **6g**. Compound **12c** exhibited the best affinity (54 nM) among them, which is 16-fold improved than **6g**. LE and FQ were also estimated for these compounds (Table 2). The continuous decrease of LE accompanied with molecular growing (Table 2), while FQ showed progressively increase (Fig. 2). Compound **12c** reached an FQ of 0.99, which is the nearest to 1.0 among all the compounds.

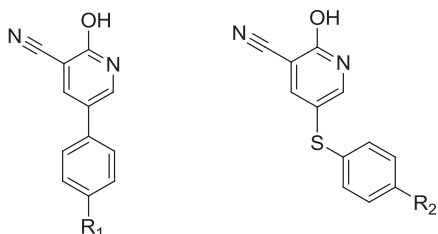
Notably, **12c** still obeys 'Rule-of-Five' (MW = 378, Clog *P* = 4.57, H-bond donors = 2, H-bond acceptors = 4). As disrupting the rigid plane structure, **12c** shows a 7-fold improved solubility (0.051 \pm 0.003 g/L) compared with **S1** (0.007 \pm 0.001 g/L).

To further identify the direct binding ability of **12c** to Mcl-1, isothermal titration calorimetry (ITC) was performed and gossypol was used as the control. **12c** exhibited a K_d value of 0.98 μ M (Fig. 3a), illustrating the binding to Mcl-1. By contrast, **12c** did not show affinity to Bcl-2 protein (Fig. 3c). In consistent with their IC₅₀ values showed in Table 2, **12c** exhibited about 2-fold higher affinity than gossypol which K_d is 2.65 μ M (Fig. 3b). Recently, studies have illustrated that the Bcl-2 and Mcl-1 protein can achieve high binding selectivity to synthetic small-molecule inhibitors due to their different flexibility and nature of their hotspots [27]. So far, we got a specific Mcl-1 inhibitor **12c**.

3.3. **12c** selectively induces apoptosis in Mcl-1-dependent cancer cells

To confirm the specificity of **12c** for the Mcl-1 protein in cellular models, we analyzed its activity in human chronic myeloid leukemia K562 cells that depend on Mcl-1 for survival and human acute leukemia RS4; 11 cells that are Bcl-2-dependent cells [28,29]. Bcl-2 specific inhibitor ABT-737 was assayed in parallel. The cell lines were treated with different concentrations of **12c** and ABT-737, respectively, and then apoptosis was determined by Annexin V flow cytometry. Fig. 4a showed western blot analysis of the expression levels of Bcl-2 and Mcl-1 in the two cell lines. As expected, ABT-737 potentially induced apoptosis in RS4; 11 cells

Table 1
Binding affinities (by FPA), LEs and FQs of compounds **2–4** and **6a–k** to Mcl-1.



Compd	R ₁	R ₂	IC ₅₀ (μ M)	K_i^a (μ M)	ΔG^b	LE ^c	FQ ^d
2	–	–	71.5 \pm 1.9	2.85 \pm 0.17	–7.62	0.42	0.83
3	–	–	1425.00 \pm 45	57.0 \pm 3.00	–5.83	0.42	0.69
4	–	–	2725.00 \pm 85	109.0 \pm 5.00	–5.44	0.60	0.82
5	–	–	No binding	No binding	–	–	–
6a	–	–	261.0 \pm 3.8	10.41 \pm 0.16	–6.85	0.46	0.79
6b	–	–	158.5 \pm 2.2	6.32 \pm 0.09	–7.14	0.38	0.77
6c	Cl	–	205.4 \pm 3.4	8.19 \pm 0.13	–6.99	0.44	0.79
6d	phenyl	–	316.2 \pm 5.2	12.60 \pm 0.21	–6.73	0.32	0.71
6e	–	H	82.2 \pm 2.5	3.29 \pm 0.10	–7.53	0.47	0.85
6f	–	methyl	63.1 \pm 2.7	2.52 \pm 0.11	–7.69	0.45	0.85
6g	–	<i>i</i> -propyl	21.5 \pm 1.8	0.86 \pm 0.07	–8.33	0.44	0.90
6h	–	<i>t</i> -amyl	177.5 \pm 5.5	7.09 \pm 0.22	–7.08	0.34	0.75
6i	–	Br	121.1 \pm 3.8	4.83 \pm 0.15	–7.30	0.43	0.81
6j	–	NH ₂	133.3 \pm 2.3	5.31 \pm 0.09	–7.25	0.43	0.80
6k	–	–	383.1 \pm 6.8	15.28 \pm 0.27	–6.61	0.29	0.69
(-)–gossypol	–	–	4.8 \pm 0.5	0.19 \pm 0.02	–9.23	0.24	0.86

^a Values were measured by FPA for inhibition constant (K_i). The values are the mean \pm SD of at least two independent experiments.

^b Free energy of binding (ΔG) was calculated as $\Delta G = -RT \ln K_i$.

^c Ligand efficiency (LE) was calculated as LE = $\Delta G/HAC$.

^d Fit quality (FQ) was calculated as Ref. [19].

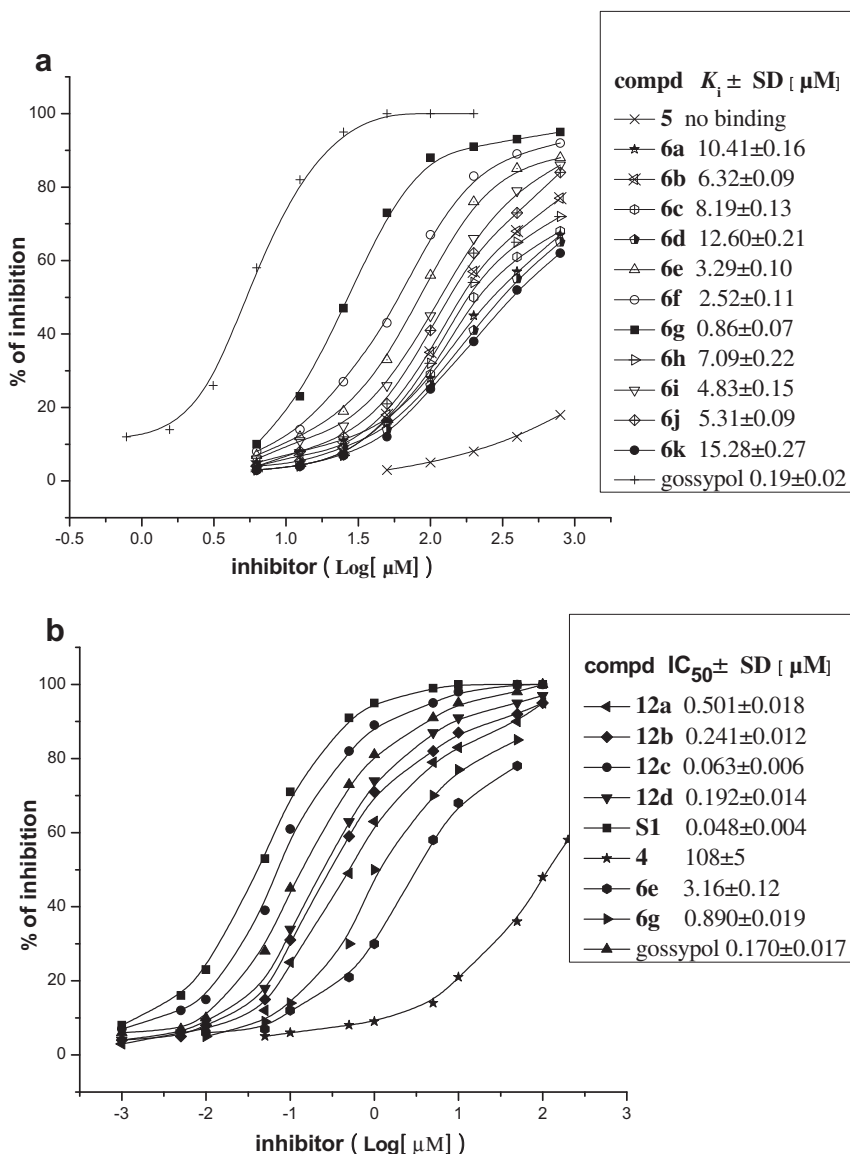


Fig. 1. Binding affinities of (a) **6a–k** to Mcl-1 by FPAs, and (b) **12a–d**, **S1**, **4**, **6e**, and **6g** a to Mcl-1 by ELISA assay. (–)gossypol as used as a control.

($IC_{50} = 0.27 \mu\text{M}$) compared to K562 cells ($IC_{50} = 16.4 \mu\text{M}$) (Fig. 4b). In contrast, treatment with **12c** markedly induced apoptosis in K562 cells ($IC_{50} = 0.84 \mu\text{M}$) with a selectivity greater than 20-fold over RS4; 11 cells ($IC_{50} = 24.5 \mu\text{M}$) (Fig. 4c), consistent with its binding selectivity for Mcl-1 over Bcl-2.

3.4. Retrospective analyses

During the fragment optimization, we encountered the expected LE dropping off as molecular size increases. This brought us a challenge to select a compound for further optimization. Guided by FQ, **6g** was identified as a relay ligand with good ligand efficiency which was more proper for further molecular growth. Based on **6g**, we got a Mcl-1 inhibitor **12c** with a much improved affinity through fragment-based molecular development.

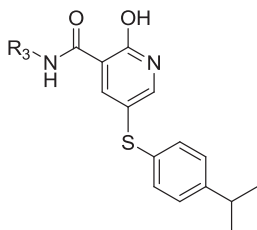
To better understand the use of the fragment-based strategy and verify the path through which we optimized here, we conducted a retrospective analysis of our hit-to-lead studies. All the compounds described here were tested by ELISA to get IC_{50} value toward Mcl-1 protein (Table 3). Free energy of binding (ΔG) was

then calculated as $\Delta G = -RT \ln IC_{50}$. ΔG was plotted against the number of heavy atoms (HAC). As shown in Fig. 5, the plot indicated that a nearly linear relationship exists between ΔG and HAC over the compounds **4**, **6e**, **6g**, and **12c**, demonstrating a reasonable lead optimization route in our hit-to-lead study. Additionally, the linear relationship between free energy and HAC in the optimization process means the ligands maintained their binding mode of the initial fragment and thus contributed additively to the final binding energy.

4. Conclusions

Utilizing our previous finding **S1** as a template, and using fragment-based strategy, we got a series of potent inhibitors of Mcl-1. The compound **12c** exhibited a nanomolar IC_{50} value (54 nM) to Mcl-1, similar to the initial compound **S1** ($IC_{50} = 46 \text{ nM}$). Excitingly, the water-solubility of **12c** is 7-fold improved than **S1**. FBDD, as illustrated in this paper, typically starts with a 'Rule-of-Three'-compliant fragment and ideally ends up with a potent 'Rule-of-Five'-compliant candidate compound. This reflected the advantages

Table 2
Binding affinities (by ELISA), LEs and FQs of compounds **12a–d**, **6g**, and **S1** to Mcl-I.



Compd	R ₃	IC ₅₀ ^a (μM)	ΔG ^b	HAC ^c	pK _i	LE ^d	FQ ^e
6g	–	0.890 ± 0.019	–8.31	19	6.05	0.44	0.90
12a	<i>i</i> -propyl	0.501 ± 0.018	–8.66	23	6.33	0.38	0.90
12b	<i>n</i> -butyl	0.241 ± 0.012	–9.09	24	6.65	0.38	0.94
12c	benzyl	0.054 ± 0.006	–9.99	27	7.27	0.37	0.99
12d	phenylpropyl	0.192 ± 0.014	–9.23	29	6.72	0.32	0.92
S1	–	0.046 ± 0.004	–10.08	24	7.34	0.42	1.04
(–)-gossypol	–	0.170 ± 0.017	–9.30	38	6.67	0.24	0.87

^a 50% Inhibitory concentration (IC₅₀). The values are the mean ± SD of at least two independent experiments.

^b Free energy of binding (ΔG) was calculated as ΔG = –RT ln IC₅₀.

^c Heavy atom count (HAC).

^d Ligand efficiency (LE) was calculated as LE = ΔG/HAC.

^e Fit quality (FQ) was calculated as Ref. [19].

of FBDD in drug discovery. Extensive studies are in progress to ascertain its therapeutic potential.

5. Experimental section

5.1. Chemistry

5.1.1. Materials and methods

All commercial reagents were purchased and used without further purification or distillation unless otherwise stated. Melting points were measured on a Griffin apparatus and are uncorrected. ¹H NMR was obtained with Bruker AV-400 spectrometer with chemical shifts reported as parts per million (in CDCl₃, TMS as internal standard). The following abbreviations are used for multiplicity of NMR signals: s = singlet, d = doublet, t = triplet, q = quartet, m = multiplet. High-resolution mass spectra (HRMS)

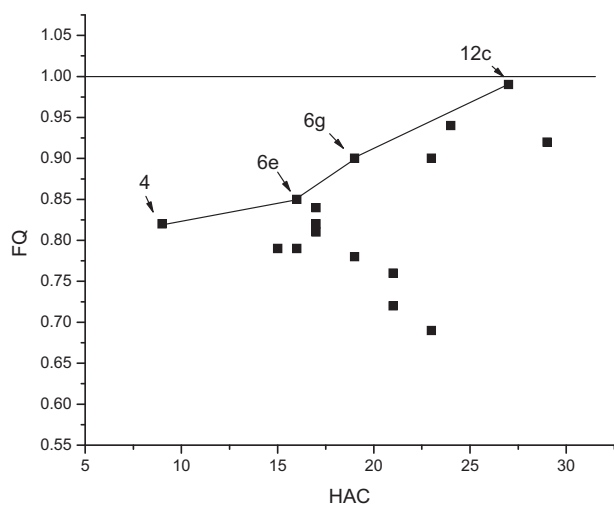


Fig. 2. FQs for all the 16 molecules composed of fragment **4** and the molecules resulting from optimization of **4**.

were obtained on HPLC-Q-T of MS (Micro) spectrometer. Column chromatography was performed on silica gel 200–300 mesh. Purity of all final products was determined by analytical HPLC to be ≥95%. HPLC purity of compounds was measured with a reverse phase HPLC (XBridge C18, 4.6 × 150 mm, 5 μm) with two diverse wavelength detection systems.

5.1.2. 2-hydroxynicotinonitrile (**4**)

A mixture of 2-chloronicotinonitrile (1.38 g, 10 mmol) and acetic acid (20 mL) was heated to 125 °C and kept for 8 h, the mixture was used in the next step without further disposal.

5.1.3. 4-methoxy-2-hydroxynicotinonitrile (**5**)

A mixture of propanedinitrile (0.33 g, 5 mmol) and trimethyl orthoformate (0.64 g, 6 mmol) was stirred for 1 h at 80 °C. The reaction was cooled to room temperature, and then added a methanol (10 mL) solution of *N,N*-dimethylformamide dimethylacetel (6 mmol) under stirring. The reaction mixture was refluxed 30 min. After cooling, the precipitates obtained were filtered, dried and recrystallized from methanol to give pure 1,1-dicyano-2-methoxy-4-dimethylamino-1,3-butadiene as light red crystals. Yield: 76%. m.p. 130–131 °C.

Acetic acid (10 mL) was added to the intermediate of last step (0.53 g, 3 mmol), the temperature raised to 125 °C until the reaction had reached completion, as monitored by TLC. The excess acetic acid was evaporated under vacuum to give the crude 4-methoxy-2-hydroxynicotinonitrile. The crude product was recrystallized from methanol to give white crystals.

Yield: 410 mg, 91%. ¹H NMR (400 MHz, CDCl₃): δ: 12.24 (s, 1H, Ar–OH), 7.64 (d, *J* = 7.6 Hz, 1H, Ar–H), 6.21 (d, *J* = 7.6 Hz, 1H, Ar–H), 4.04 (s, 3H, CH₃).

5.1.4. 5-bromo-2-hydroxynicotinonitrile (**1**)

Bromine (2 mL, 39.1 mmol) was slowly dropped to acetic acid solution (the mixture of last step) of 2-hydroxynicotinonitrile (**4**) at room temperature within 0.5 h, kept stirring for 3 h. Then the solution of sodium pyrosulfite (20%, 20 mL) was added. The mixed was extracted with CH₂Cl₂ (3 × 20 mL). The organic layer was washed with brine and dried with MgSO₄. The solvent was removed under reduced pressure to give a white solid 1.1 g.

5.1.5. General procedure for the preparation of **6a** and **6b**

A mixture of dimethylformamide (1.96 g, 27 mmol) and phosphoryl chloride (2.47 g, 16 mmol) and corresponding acetic acid (5.4 mmol) was stirred for 3 h at 80 °C. The mixture was put on ice (30 g) and conc. NaClO₄ solution was added. The resulting precipitate was filtered off and washed with diluted NaClO₄ solution. The product was used in the next step without further disposal. It was added to a solution of sodium methoxide (0.162 g, 3.0 mmol) in 13 mL of CH₃OH. Then cyanoacetamide (0.10 g, 3.28 mmol) was added. The mixture was stirred at room temperature for 2 h and then refluxed 3 h during which time a yellow solid separated. Water was added, and the mixture was acidified and filtered to remove a yellow solid which was washed with water, ethanol, ether, and then hexane to give crude product. The crude product was recrystallized from ethanol.

5.1.5.1. 5-phenyl-2-hydroxynicotinonitrile (6a). Yield: 392 mg, 61%. ¹H NMR (400 MHz, CDCl₃): δ: 12.97 (s, 1H, Ar–OH), 8.30 (s, 1H, Ar–H), 8.02 (s, 1H, Ar–H), 7.49–7.52 (d, *J* = 8.0 Hz, 2H), 7.41–7.43 (m, 3H, Ar–H). TOF MS (EI⁺): C₁₂H₈N₂O, calcd for 196.0637, found 196.0639.

5.1.5.2. 5-naphthyl-2-hydroxynicotinonitrile (6b). Yield: 250 mg, 31%. ¹H NMR (400 MHz, CDCl₃): δ: 13.42 (s, 1H, Ar–OH), 8.14 (s, 1H,

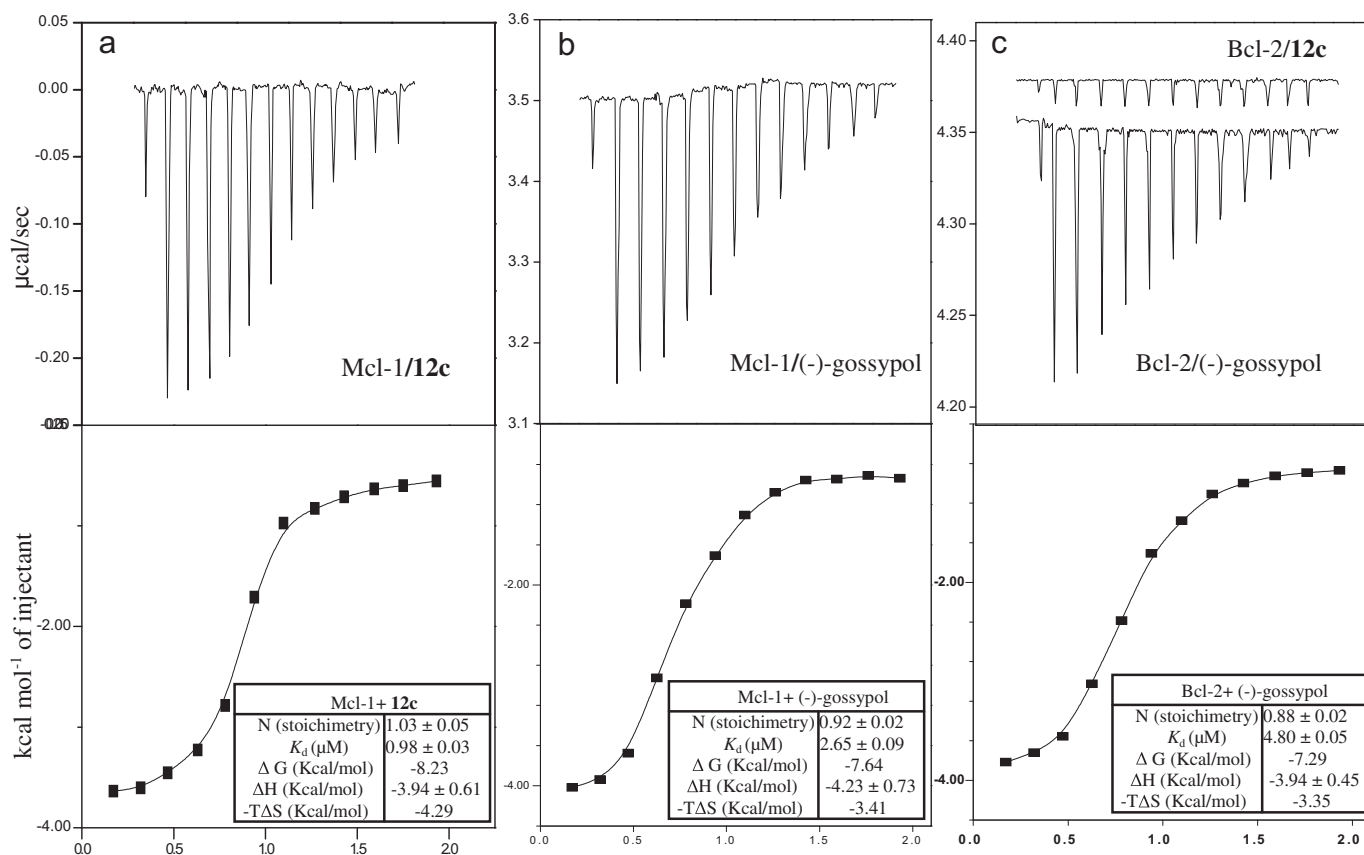


Fig. 3. The binding affinities determined by ITC of **12c** to Mcl-1 and Bcl-2 protein, respectively. (a) Raw data for titration of **12c** into Mcl-1. (b) Raw data for titration of gossypol into Mcl-1. (c) Raw data for titration of **12c** and gossypol respectively into Bcl-2. The upper panels display the raw titration data. Each point on the curves in the lower panels represents the integration of the area of the inflection produced by each injection.

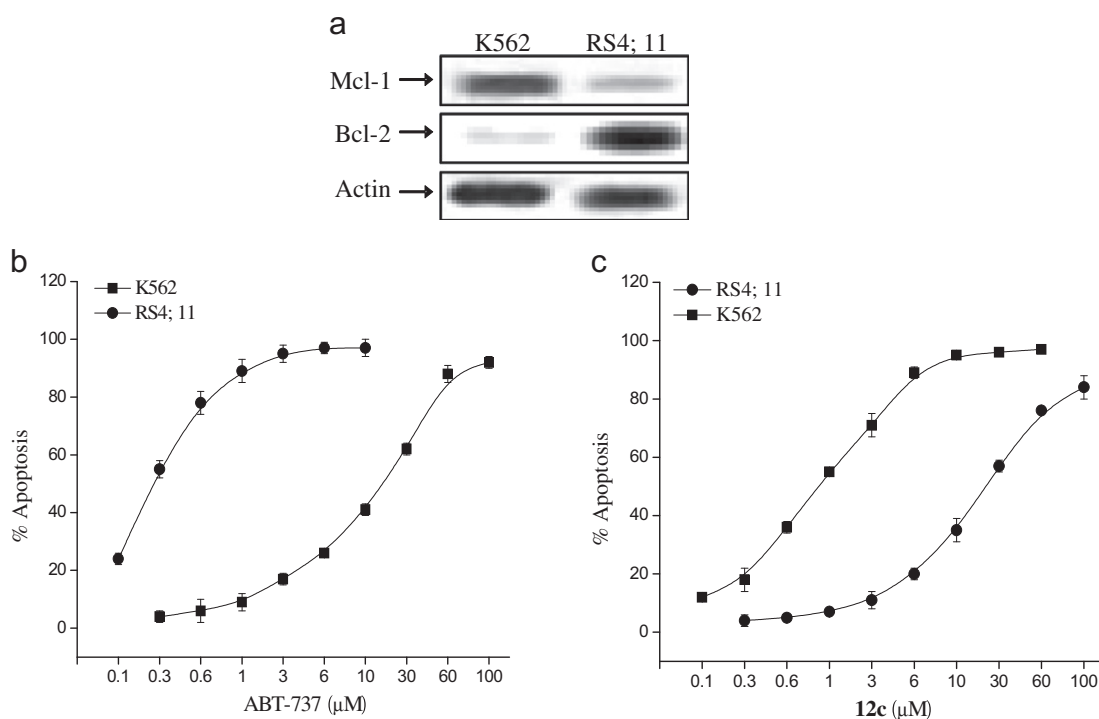


Fig. 4. Apoptosis induction of **12c** in Mcl-1-dependent cells. (a) The levels of Mcl-1 and Bcl-2 protein in K562 and RS4; 11 cells were examined by western blot. (b, c) Cells were treated with graded concentration of ABT-737 or **12c** for 48 h, and then the percentage of apoptotic cells was determined by Annexin V flow cytometry.

Table 3
Binding affinities (by ELISA) of compounds **4**, **6a–k** and **12a–d** to Mcl-I.

Compd	IC ₅₀ ^a (μM)	ΔG ^b	HAC ^c	Compd	IC ₅₀ ^a (μM)	ΔG ^b	HAC ^c
4	103 ± 5	-5.51	9	6i	4.39 ± 0.07	-7.36	17
6a	9.16 ± 0.12	-6.92	15	6j	4.93 ± 0.11	-7.29	17
6b	5.31 ± 0.09	-7.25	19	6k	13.64 ± 0.12	-6.68	23
6c	7.59 ± 0.08	-7.03	16	12a	0.501 ± 0.018	-8.66	23
6d	11.22 ± 0.11	-6.80	21	12b	0.241 ± 0.012	-9.09	24
6e	3.16 ± 0.12	-7.56	16	12c	0.054 ± 0.006	-9.99	27
6f	2.93 ± 0.04	-7.60	17	12d	0.192 ± 0.014	-9.23	29
6g	0.89 ± 0.02	-8.31	19	(-)-gossypol	0.170 ± 0.017	-9.30	38
6h	6.21 ± 0.14	-7.15	21				

^a Same as in Table 2.^b Same as in Table 2.^c Heavy atom count (HAC).

Ar–H), 7.93–7.97 (m, 2H, Ar–H), 7.88 (s, 1H, Ar–H), 7.74–7.76 (t, 1H, Ar–H), 7.53–7.59 (t, 3H, Ar–H), 7.37–7.39 (d, $J = 8.0$ Hz, 1H, Ar–H). TOF MS (EI⁺): C₁₆H₁₀N₂O, calcd for 246.0793, found 246.0797.

5.1.6. General procedure for the preparation of **6c** and **6d**

5-bromo-2-hydroxynicotinonitrile (**1**) (398 mg, 2 mmol), corresponding boronic acid (2.2 eq) were dissolved in a mixture of toluene/acetonitrile (95:5) (10 mL). Potassium tert-butoxide (3 eq) and tetrakis(triphenylphosphine)palladium(0) (0.05 eq) were added and degassed using nitrogen. The mixture was stirred for a further 10 min while purging with nitrogen. The vial was sealed and heated at 110 °C for 12–16 h. The solvent was removed in vacuo and the water (20 mL) was added. The solution was extracted with ethyl acetate (3 × 20 mL). The organic layer was collected and dried with anhydrous MgSO₄. After evaporation under reduced pressure, the product was purified by column chromatography on silica gel using dichloromethane/methanol (20:1).

5.1.6.1. 5-(4-chlorophenyl)-2-hydroxynicotinonitrile (6c). Yield: 246 mg, 53%. ¹H NMR (400 MHz, CDCl₃): δ: 12.92 (s, 1H, Ar–OH), 8.60 (s, 1H, Ar–H), 8.17 (s, 1H, Ar–H), 7.66–7.68 (d, $J = 8.4$ Hz, 2H, Ar–H), 7.47–7.49 (d, $J = 8.4$ Hz, 2H, Ar–H). TOF MS (EI⁺): C₁₂H₇ClN₂O, calcd for 230.0247, found 230.0241.

5.1.6.2. 5-(4-biphenyl)-2-hydroxynicotinonitrile (6d). Yield: 280 mg, 79%. ¹H NMR (400 MHz, DMSO-d₆): δ: 12.90 (s, 1H, Ar–OH), 8.64 (s,

1H, Ar–H), 8.19 (s, 1H, Ar–H), 7.70–7.74 (m, 5H, Ar–H), 7.46–7.50 (t, 3H, Ar–H), 7.36–7.39 (t, 1H, Ar–H). TOF MS (EI⁺): C₁₈H₁₂N₂O, calcd for 272.0950, found 272.0954.

5.1.7. General procedure for the preparation of **6e–j**

5-bromo-2-hydroxynicotinonitrile (**1**) (199 mg, 2 mmol), Cs₂CO₃ (651 mg, 2 mmol), CuI (20 mg, 10%) was added to a solution of corresponding thiophenol (4 mmol) in acetonitrile (20 mL). Then the flask was evacuated and backfilled with N₂. The reaction mixture was refluxed overnight. The solvent was removed in vacuo and water (20 mL) was added. The solution was extracted with ethyl acetate (3 × 20 mL). Then organic layer was collected and dried with anhydrous MgSO₄. After evaporation under reduced pressure, the crude product was purified by silica gel flash column chromatography (dichloromethane/acetone, 20:1).

5.1.7.1. 5-phenylthio-2-hydroxynicotinonitrile (6e). Yield: 169 mg, 37%. ¹H NMR (400 MHz, CDCl₃): δ: 12.95 (s, 1H, Ar–OH), 8.30 (s, 1H, Ar–H), 8.10 (s, 1H, Ar–H), 7.31–7.35 (m, 2H, Ar–H), 7.20–7.24 (m, 3H, Ar–H). TOF MS (EI⁺): C₁₂H₈N₂OS, calcd for 228.0357, found 228.0355.

5.1.7.2. 5-(4-methylthiophenol)-2-hydroxynicotinonitrile (6f). Yield: 256 mg, 53%. ¹H NMR (400 MHz, CDCl₃): δ: 12.89 (s, 1H, Ar–OH), 8.21 (s, 1H, Ar–H), 8.05 (s, 1H, Ar–H), 7.18–7.20 (d, $J = 7.2$ Hz, 2H, Ar–H), 7.15–7.17 (d, $J = 7.2$ Hz, 2H, Ar–H), 1.16 (m, 3H, CH₃). TOF MS (EI⁺): C₁₃H₁₀N₂OS, calcd for 242.0514, found 242.0517.

5.1.7.3. 5-(4-isopropylthiophenol)-2-hydroxynicotinonitrile (6g). Yield: 345 mg, 60%. ¹H NMR (400 MHz, CDCl₃): δ: 12.93 (s, 1H, Ar–OH), 8.29 (s, 1H, Ar–H), 8.06 (s, 1H, Ar–H), 7.20–7.22 (d, $J = 8.0$ Hz, 2H, Ar–H), 7.17–7.19 (d, $J = 8.0$ Hz, 2H, Ar–H), 1.16–1.17 (m, 1H, CH), 1.16 (s, 6H, CH(CH₃)₂). TOF MS (EI⁺): C₁₅H₁₄N₂OS, calcd for 270.0827, found 270.0823.

5.1.7.4. 5-(4-tert-amylthiophenol)-2-hydroxynicotinonitrile (6h). Yield: 245 mg, 41%. ¹H NMR (400 MHz, CDCl₃): δ: 12.98 (s, 1H, Ar–OH), 8.24 (s, 1H, Ar–H), 8.13 (s, 1H, Ar–H), 7.26–7.28 (d, $J = 8.0$ Hz, 2H, Ar–H), 7.05–7.07 (d, $J = 8.0$ Hz, 2H, Ar–H), 1.28–1.31 (m, 2H, CH₂), 0.96 (s, 6H, C(CH₃)₂), 0.91 (t, 3H, CH₂CH₃). TOF MS (EI⁺): C₁₇H₁₈N₂OS, calcd for 298.1140, found 298.1143.

5.1.7.5. 5-(4-bromophenylthio)-2-hydroxynicotinonitrile (6i). Yield: 325 mg, 53%. ¹H NMR (400 MHz, CDCl₃): δ: 12.69 (s, 1H, Ar–OH), 8.21 (s, 1H, Ar–H), 8.10 (s, 1H, Ar–H), 7.48–7.50 (d, $J = 8.4$ Hz, 2H, Ar–H), 7.16–7.19 (d, $J = 8.4$ Hz, 2H, Ar–H). TOF MS (EI⁺): C₁₂H₇BrN₂O, calcd for 305.9462, found 305.9459.

5.1.7.6. 5-(4-aminophenylthio)-2-hydroxynicotinonitrile (6j). Yield: 204 mg, 42%. ¹H NMR (400 MHz, CDCl₃): δ: 12.73 (s, 1H, Ar–OH), 8.15 (s, 1H, Ar–H), 7.81 (s, 1H, Ar–H), 7.14–7.16 (d, $J = 7.2$ Hz, 2H, Ar–H), 6.53–6.55 (d, $J = 7.2$ Hz, 2H, Ar–H), 5.39 (m, 2H, NH₂). TOF MS (EI⁺): C₁₂H₉N₃OS, calcd for 243.0466, found 243.0463.

5.1.8. 1-benzyl-5-(4-isopropylphenylthio)-2-oxo-1,2-dihydropyridine-3-carbonitrile (6k)

To a solution of 5-(4-isopropylthiophenol)-2-hydroxynicotinonitrile (**6g**, 200 mg, 0.74 mmol) in acetonitrile (10 mL) was added anhydrous K₂CO₃ (306 mg, 2.2 mmol, 3 eq) and benzyl bromide (165 mg, 0.96 mmol, 1.3 eq). The reaction was carried out under N₂ atmosphere. The solution was heated at 100 °C for 12 h. The reaction was then cooled to room temperature and filtered through a pad of celite. The filtrate was then concentrated in vacuo. Subsequently, crude product was purified by silica gel flash column chromatography (dichloromethane/acetone, 60:1) afforded the

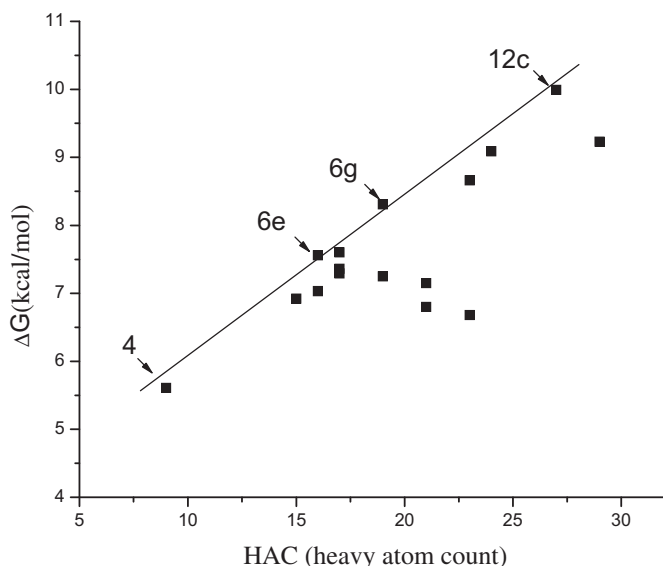


Fig. 5. Relationship between free energy of binding (in kcal/mol) ($\Delta G = -RT \ln IC_{50}$) and HAC (heavy atom count) of all the 16 compounds.

desired compound. Yield: 120 mg, 45%. $^1\text{H NMR}$ (400 MHz, CDCl_3): δ : 7.99 (s, 1H, Ar–H), 7.56 (s, 1H, Ar–H), 7.33–7.35 (d, $J = 8.4$ Hz, 2H, Ar–H), 7.21–7.23 (m, 3H, Ar–H), 7.14–7.16 (d, $J = 7.6$ Hz, 2H, Ar–H), 6.87–6.89 (d, $J = 8.0$ Hz, 2H, Ar–H), 4.98 (s, 2H, CH_2), 1.26–1.27 (m, 1H, CH), 1.19 (s, 6H, $\text{CH}(\text{CH}_3)_2$). TOF MS (EI^+): $\text{C}_{22}\text{H}_{20}\text{N}_2\text{O}_5$, calcd for 360.1296, found 360.1290.

5.1.9. 2-chloronicotinic acid (7)

A solution of the 2-chloronicotinonitrile (4.14 g, 30 mmol) in 30 mL of 50% sulfuric acid was heated for at 100 °C for 10 h and then the reaction mixture was poured into the crushed ice. The resultant precipitate was filtered, washed with water and dried. The solid was recrystallized from 90% ethanol. Yield: 4.16 g, 88%.

5.1.10. 2-chloronicotinoylchloride (8)

A solution of 2-chloronicotinic acid (7) (1 g, 6.3 mmol), a catalytic amount of anhydrous DMF (0.13 mmol, 10 μL), and thionyl chloride (15 mL) was heated at reflux for 6 h. The reaction mixture was cooled to room temperature and the excess of thionyl chloride was removed under reduced pressure. The acid chloride thus formed and the mixture was used in the next step without further disposal.

5.1.11. General procedure for the preparation of 9a–d

The mixture of 2-chloronicotinoylchloride (8) in last step was dissolved in anhydrous CH_2Cl_2 (10 mL) and then added dropwise to a CH_2Cl_2 (10 mL) solution of the corresponding amine (15 mmol) cooled at 0 °C under stirring. The mixture was allowed to warm to room temperature and stirring was continued for additional 4 h. After treatment of the reaction mixture with a 5% solution of sodium hydroxide (15 mL) and separation of the organic layer, the aqueous phase was extracted with ethyl acetate (3 \times 15 mL) to recover further product. The combined organic extracts were dried (Na_2SO_4) and evaporated under reduced pressure. The residue was purified by flash chromatography on silica gel using dichloromethane/acetone (30:1).

5.1.11.1. *N*-isopropyl-2-chloronicotinamide (9a). Yield: 898 mg, 72%. $^1\text{H NMR}$ (400 MHz, CDCl_3): δ 8.44–8.46 (d, $J = 8.4$ Hz, 1H, Ar–H), 8.10–8.12 (d, $J = 9.2$ Hz, 1H, Ar–H), 7.34 (m, 1H, Ar–H), 6.47 (s, 1H, NH), 2.84 (m, 1H, CH), 1.24 (s, 6H, $(\text{CH}_3)_2$). TOF MS (EI^+): $\text{C}_9\text{H}_{11}\text{ClN}_2\text{O}$, calcd for 198.0560, found 198.0562.

5.1.11.2. *N*-butyl-2-chloronicotinamide (9b). Yield: 935 mg, 70%. $^1\text{H NMR}$ (400 MHz, CDCl_3): δ 8.40–8.42 (d, $J = 8.0$ Hz, 1H, Ar–H), 7.98–8.01 (d, $J = 9.2$ Hz, 1H, Ar–H), 7.33–7.36 (m, 1H, Ar–H), 6.42 (s, 1H, NH), 3.47–3.52 (t, 2H, CH_2), 1.60–1.67 (m, 2H, CH_2), 1.42–1.47 (m, 2H, CH_2), 0.96–0.99 (t, 3H, CH_3). TOF MS (EI^+): $\text{C}_{10}\text{H}_{13}\text{ClN}_2\text{O}$, calcd for 212.0716, found 212.0720.

5.1.11.3. *N*-benzyl-2-chloronicotinamide (9c). Yield: 1224 mg, 79%. $^1\text{H NMR}$ (400 MHz, CDCl_3): δ 9.74–9.75 (d, $J = 6.4$ Hz, 1H, Ar–H), 8.61–8.62 (d, $J = 8.4$ Hz, 1H, Ar–H), 8.26–8.29 (m, 1H, Ar–H), 7.49 (s, 1H, NH), 7.34–7.35 (m, 2H, Ar–H), 7.26–7.29 (m, 3H, Ar–H), 4.66–4.67 (s, 2H, CH_2). TOF MS (EI^+): $\text{C}_{13}\text{H}_{11}\text{ClN}_2\text{O}$, calcd for 246.0560, found 246.0563.

5.1.11.4. *N*-phenylpropyl-2-chloronicotinamide (9d). Yield: 1191 mg, 69%. $^1\text{H NMR}$ (400 MHz, CDCl_3): δ 9.48–9.49 (d, $J = 6.4$ Hz, 1H, Ar–H), 8.26–8.27 (d, $J = 4.8$ Hz, 1H, Ar–H), 7.94–7.99 (m, 1H, Ar–H), 7.72 (s, 1H, NH), 7.44–7.45 (m, 2H, Ar–H), 7.36–7.38 (m, 3H, Ar–H), 3.24–3.27 (t, 2H, CH_2), 2.59–2.62 (m, 2H, CH_2), 1.73–1.77 (t, 2H, CH_2). TOF MS (EI^+): $\text{C}_{15}\text{H}_{15}\text{ClN}_2\text{O}$, calcd for 274.0873, found 274.0869.

5.1.12. General procedure for the preparation of 11a–d

Acetic acid (20 mL) was added to corresponding 2-chloronicotinamide (9a–d) (2 mmol), the temperature raised to 125 °C until the reaction had reached completion, as monitored by TLC. The corresponding desired crude intermediates (10a–d) were obtained and the mixture was used in the next step without further disposal. The resulting mixture was cooled to room temperature. Bromine (0.5 mL, 9.5 mmol) was slowly dropped to acetic acid solution of (10a–d) at room temperature within 0.5 h, kept stirring for 3 h. Then the solution of sodium pyrosulfite (20%, 10 mL) was added. The mixed was extracted with CH_2Cl_2 (3 \times 20 mL). The organic layer was washed with brine and dried with MgSO_4 . Concentration of the organic layer afforded the desired crude product. Purification by silica gel flash column chromatography (dichloromethane/methanol, 20:1) afforded the desired compound.

5.1.12.1. *N*-isopropyl-5-bromo-2-hydroxynicotinamide (11a). Yield: 275 mg, 53%. $^1\text{H NMR}$ (400 MHz, CDCl_3): δ 12.88 (s, 1H, Ar–OH), 9.56 (s, 1H, N–H), 8.27 (s, 1H, Ar–H), 7.99 (s, 1H, Ar–H), 3.99–4.04 (m, 1H, CH), 1.15 (s, 6H, $(\text{CH}_3)_2$). TOF MS (ESI): $\text{C}_9\text{H}_{11}\text{BrN}_2\text{O}_2$, for $[\text{M} + \text{H}]^+$, calcd for 259.0082, found 259.0078.

5.1.12.2. *N*-butyl-5-bromo-2-hydroxynicotinamide (11b). Yield: 251 mg, 46%. $^1\text{H NMR}$ (400 MHz, CDCl_3): δ 12.87 (s, 1H, Ar–OH), 9.64 (s, 1H, N–H), 8.27 (s, 1H, Ar–H), 7.99 (s, 1H, Ar–H), 3.27–3.33 (t, 2H, CH_2), 1.44–1.51 (m, 2H, CH_2), 1.29–1.36 (m, 2H, CH_2), 0.88–0.91 (t, 3H, CH_3). TOF MS (ESI): $\text{C}_{10}\text{H}_{13}\text{BrN}_2\text{O}_2$, for $[\text{M} + \text{H}]^+$, calcd for 273.0239, found 273.0245.

5.1.12.3. *N*-benzyl-5-bromo-2-hydroxynicotinamide (11c). Yield: 417 mg, 68%. $^1\text{H NMR}$ (400 MHz, CDCl_3): δ 12.53 (s, 1H, Ar–OH), 9.74 (s, 1H, N–H), 8.71 (s, 1H, Ar–H), 7.58 (s, 1H, Ar–H), 7.34–7.36 (m, 2H, Ar–H), 7.26–7.30 (m, 3H, Ar–H), 4.68 (s, 2H, CH_2). TOF MS (ESI): $\text{C}_{13}\text{H}_{11}\text{BrN}_2\text{O}_2$, for $[\text{M} + \text{H}]^+$, calcd for 307.0082, found 307.0086.

5.1.12.4. *N*-phenylpropyl-5-bromo-2-hydroxynicotinamide (11d). Yield: 382 mg, 57%. $^1\text{H NMR}$ (400 MHz, CDCl_3): δ 12.87 (s, 1H, Ar–OH), 9.68 (s, 1H, Ar–H), 8.26 (s, 1H, Ar–H), 7.99 (s, 1H, N–H), 7.44–7.47 (m, 2H, Ar–H), 7.17–7.20 (m, 3H, Ar–H), 3.26–3.33 (t, 2H, CH_2), 2.57–2.61 (m, 2H, CH_2), 1.77–1.80 (t, 2H, CH_2). TOF MS (ESI): $\text{C}_{15}\text{H}_{15}\text{BrN}_2\text{O}_2$, for $[\text{M} + \text{H}]^+$, calcd for 335.0395, found 335.0391.

5.1.13. General procedure for the preparation of 12a–d

Corresponding 5-bromo-2-hydroxynicotinonitrile (11a–d) (1 mmol), Potassium tert-butoxide (3 eq) and tetrakis(triphenylphosphine)palladium(0) (0.05 eq), CuI (20 mg) was added to a flask. Then the flask was evacuated and backfilled with N_2 . 4-isopropyl thiophenol (3 eq) and DMF (10 mL) were added under argon atmosphere. The reaction mixture was refluxed overnight. The solvent was removed under reduced pressure and the water (20 mL) was added. The solution was extracted with dichloromethane (3 \times 20 mL). The organic layer was collected and dried with anhydrous MgSO_4 , and concentrated in vacuo to give the crude product. Purification by silica gel flash column chromatography (dichloromethane/methanol, 30:1) afforded the desired compound.

5.1.13.1. *N*-isopropyl-5-(4-isopropylthiophenol)-2-hydroxynicotinamide (12a). Yield: 116 mg, 35%. $^1\text{H NMR}$ (400 MHz, CDCl_3): δ 12.68 (s, 1H, Ar–OH), 9.23 (s, 1H, N–H), 8.69 (s, 1H, Ar–H), 7.67 (s, 1H, Ar–H), 7.19–7.21 (d, $J = 8.0$ Hz, 2H, Ar–H), 7.14–7.16 (d, $J = 8.0$ Hz, 2H, Ar–H), 4.21–4.25 (m, 1H, CH), 2.83–2.90 (m, 1H, CH), 1.23–1.25 (d, 6H, $\text{CH}(\text{CH}_3)_2$), 1.20–1.21 (d, 6H, $(\text{CH}_3)_2$). TOF MS (ESI): $\text{C}_{18}\text{H}_{22}\text{N}_2\text{O}_2\text{S}$, for $[\text{M} + \text{H}]^+$, calcd for 331.1480, found 331.1481.

5.1.13.2. *N*-butyl-5-(4-isopropylthiophenol)-2-hydroxynicotinamide (**12b**). Yield: 97 mg, 28%. ^1H NMR (400 MHz, CDCl_3): δ 12.19 (s, 1H, Ar–OH), 9.37 (s, 1H, N–H), 8.68 (s, 1H, Ar–H), 7.69 (s, 1H, Ar–H), 7.20–7.22 (d, $J = 8.4$ Hz, 2H, Ar–H), 7.14–7.16 (d, $J = 8.4$ Hz, 2H, Ar–H), 3.41–3.49 (t, 2H, CH_2), 1.58–1.61 (m, 2H, CH_2), 1.38–1.43 (m, 2H, CH_2), 0.93–0.97 (t, 3H, CH_3), 2.83–2.90 (m, 1H, CH), 1.20–1.23 (d, 6H, $\text{CH}(\text{CH}_3)_2$). TOF MS (ESI): $\text{C}_{19}\text{H}_{24}\text{N}_2\text{O}_2\text{S}$, for $[\text{M} + \text{H}]^+$, calcd for 345.1637, found 345.1643.

5.1.13.3. *N*-benzyl-5-(4-isopropylthiophenol)-2-hydroxynicotinamide (**12c**). Yield: 144 mg, 38%. ^1H NMR (400 MHz, CDCl_3): δ 12.50 (s, 1H, Ar–OH), 9.77 (s, 1H, N–H), 8.70 (s, 1H, Ar–H), 7.65 (s, 1H, Ar–H), 7.32–7.33 (m, 2H, Ar–H), 7.26–7.27 (m, 3H, Ar–H), 7.19–7.21 (d, $J = 8.0$ Hz, 2H, Ar–H), 7.13–7.15 (d, $J = 8.0$ Hz, 2H, Ar–H), 4.65 (s, 2H, CH_2), 2.84–2.87 (m, 1H, CH), 1.19–1.21 (d, 6H, $\text{CH}(\text{CH}_3)_2$). TOF MS (ESI): $\text{C}_{22}\text{H}_{22}\text{N}_2\text{O}_2\text{S}$, for $[\text{M} + \text{H}]^+$, calcd for 379.1480, found 379.1474.

5.1.13.4. *N*-phenylpropyl-5-(4-isopropylthiophenol)-2-hydroxynicotinamide (**12d**). Yield: 118 mg, 29%. ^1H NMR (400 MHz, CDCl_3): δ 12.89 (s, 1H, Ar–OH), 9.70 (s, 1H, N–H), 8.20 (s, 1H, Ar–H), 7.99 (s, 1H, Ar–H), 7.56–7.58 (d, $J = 7.6$ Hz, 2H, Ar–H), 7.35–7.37 (d, $J = 8.0$ Hz, 2H, Ar–H), 7.28–7.29 (m, 2H, Ar–H), 7.18–7.23 (m, 3H, Ar–H), 2.70–2.72 (t, 2H, CH_2), 2.08–2.10 (m, 2H, CH_2), 1.76–1.80 (t, 2H, CH_2), 2.82–2.86 (m, 1H, CH), 1.15–1.17 (d, 6H, $\text{CH}(\text{CH}_3)_2$). TOF MS (ESI): $\text{C}_{24}\text{H}_{26}\text{N}_2\text{O}_2\text{S}$, for $[\text{M} + \text{H}]^+$ calcd for 407.1793, found 407.1799.

5.2. Binding affinity assay

5.2.1. Reagents

A 21-residue Bid BH3 peptide (residues 79–99) bearing a 6-carboxy-fluorescein succinimidyl ester fluorescence tag (FAM-Bid) was synthesized at HD Biosciences (Shanghai, China). Recombinant protein of Bcl-2 and Mcl-1 was synthesized and purified from bacteria of *Escherichia coli* BL21 as described in our previous study [8,30].

5.2.2. Fluorescence polarization-based binding assay (FPA)

For the competitive binding assay for Bcl-2 protein, FAM-Bid peptide (5 nM) and Bcl-2 protein (40 nM) were preincubated in the assay buffer (100 mM potassium phosphate, pH 7.5; 100 $\mu\text{g}/\text{mL}$ bovine gamma globulin; 0.02% sodium azide). Each inhibitor was first dissolved in pure DMSO to obtain a 4 mM stock solution. Then the stock solution was diluted successively to get the solution with different concentration gradients (400 μM , 200 μM , 100 μM , 50 μM , 25 μM , 12.5 μM , 6.25 μM , 3.125 μM , 1.5625 μM and 0.78125 μM). Next, serial dilutions of compounds were added. After 30 min incubation, the polarization values were measured using the Spectra Max M5 Detection System in a black 96-well plate. Saturation experiments determined that FAM-Bid binds to the Bcl-2 protein with a K_d value of 8 nM. For Mcl-1, assays were performed in the same manner as that for Bcl-2 with the following exceptions: 50 nM Mcl-1 and 10 nM FAM-Bid peptide were used in the assay buffer (25 mM Tris, pH 8.0; 150 mM NaCl). FAM-Bid peptide binds to the Mcl-1 protein with a K_d value of 1.9 nM. (-)-gossypol was used as comparison in our assay. The K_i value for each inhibitor was calculated using the equation Wang et al. have developed for FP-based assays [31]. The computer program for calculating K_i values for FP-based assays is available free of charge at: http://sw16.im.med.umich.edu/software/calc_ki/.

5.2.3. Enzyme-linked immunosorbent assay (ELISA)

An enzyme-linked immunosorbent assay was reported as previous [30]. For this assay, biotinylated Bim peptide (residues

81–106, biotin-(β)A-(β)A-D-M-R-P-E-I-W-I-A-Q-E-L-R-R-I-G-D-E-F-N-A-Y-Y-A-R-R-amide, hereafter called biotin-Bim) was diluted to 0.09 $\mu\text{g}/\text{mL}$ in SuperBlock blocking buffer in PBS (Pierce Biotechnology, Inc, Rockford, IL, catalog #37515) and incubated for 1.5 h in 96-well microtiter plates already coated with streptavidin (Qiagen, Catalog #15500) to allow the formation of the complex between Biotin-Bim and streptavidin. All incubations were performed at room temperature unless otherwise noted. Each inhibitor was first dissolved in pure DMSO to obtain a 10 mM stock solution. Then the stock solution was diluted successively to get the solution with different concentration gradients (200 μM , 100 μM , 10 μM , 5 μM , 1 μM , 0.5 μM , 0.1 μM , 0.05 μM , 0.01 μM , 0.005 μM , and 0.001 μM). For each tested inhibitor, different concentrations of the inhibitor were incubated with 20 nM His-tagged Mcl-1 protein in PBS for 1 h with a final DMSO concentration of 4%. The plates were washed three times with PBS containing 0.05% Tween-20. The inhibitor and protein mixture (100 μL) was transferred to the plate containing the biotin-Bim/streptavidin complex and incubated for 2 h. The plate was then washed as before and mouse anti-His antibody that conjugated with horseradish peroxidase (Qiagen, Catalog #34460) was added into the wells and incubated for 1 h. The plate was then washed with PBS containing 0.05% Tween-20. Finally, TMB (100 μL , Beyotime, Catalog #P0209) was added to each well; the enzymatic reaction was stopped after 30 min by addition of H_2SO_4 (100 μL , 2 M). Absorbances were measured with a TECAN GENios (Swiss, TECAN) microplate reader using a wavelength of 450 nm. Three independent experiments were performed with each inhibitor to calculate average IC_{50} value and standard deviation (SD). (-)-gossypol was used as comparison in our assay.

5.2.4. Isothermal titration calorimetry (ITC) assay

Isothermal titration calorimetry (ITC) was performed using iTC200 (Microcal). Experiments were performed in 20 mM Tris pH 8.0, 150 mM NaCl, 1% DMSO at 25 $^{\circ}\text{C}$. For evaluating K_d value of **12c**, titrations consisted of 12×3 μL injections of compound at 300 μM into Mcl-1 (30 μM). All sample data obtained after control data corrections were analyzed to fit to a one-site model. For control ITC experiments, the sample cells were filled with assay buffer and the compound solution was added. This process was identical to that for protein samples.

5.2.5. The measure of compounds solubility

An aqueous solubility study was carried out in distilled water according to Lipinski. In brief, an excess amount of compounds (20 mg) was added to 100 mL of distilled water. Flasks were sealed and shaken at 25 $^{\circ}\text{C}$ for 48 h in the dark. After equilibrium was reached, the solution was filtered through a 0.45 μm hydrophilic membrane filter with the first one-third of the solution being discarded. The concentration of **12c** and **S1** in the filtrate was determined by a UV–vis spectrophotometer at 592 nm (HP 8453 spectrophotometer, HP, USA). Three independent experiments were performed with each inhibitor to calculate average solubility and standard deviation (SD).

5.3. Cell culture and assessment of apoptosis

RS4; 11 cell line and K562 cell line were purchased from China Center for Type Culture Collection (Wuhan, China). Cells were cultured routinely. Apoptosis was determined by flow cytometric measurement of phosphatidylserine exposure using Annexin V FITC. Cells were washed twice with PBS and incubated with a 1:40 solution of FITC-conjugated Annexin V for 10 min at room temperature. Stained cells were analyzed by flow cytometry.

Acknowledgments

This work was partly supported by the National Natural Science Foundation of China (81273436, 81272876).

References

- [1] J.M. Adams, S. Cory, The Bcl-2 protein family: arbiters of cell survival, *Science* 281 (1998) 1322–1326.
- [2] D.T. Chao, S.J. Korsmeyer, Bcl-2 family: regulators of cell death, *Annu. Rev. Immunol.* 16 (1998) 395–419.
- [3] A.J. Minn, R.E. Swain, A. Ma, C.B. Thompson, Recent progress on the regulation of apoptosis by Bcl-2 family members, *Adv. Immunol.* 70 (1998) 245–279.
- [4] S.N. Willis, J.M. Adams, Life in the balance: how BH3-only proteins induce apoptosis, *Curr. Opin. Cell. Biol.* 17 (2005) 617–625.
- [5] M.R. Warr, G.C. Shore, Unique biology of Mcl-1: therapeutic opportunities in cancer, *Curr. Mol. Med.* 8 (2008) 138–147.
- [6] P.H. Bernardo, T. Sivaraman, K.F. Wan, J. Xu, J. Krishnamoorthy, C.M. Song, L. Tian, J.S.F. Chin, D.S.W. Lim, H.Y.K. Mok, V.C. Yu, J.C. Tong, C.L.L. Chai, Structural insights into the design of small molecule inhibitors that selectively antagonize Mcl-1, *J. Med. Chem.* 53 (2010) 2314–2318.
- [7] E.F. Lee, P.E. Czabotar, M.F. van Delft, E.M. Michalak, M.J. Boyle, S.N. Willis, H. Puthalakath, P. Bouillet, P.M. Colman, D.C.S. Huang, W.D. Fairlie, A novel BH3 ligand that selectively targets Mcl-1 reveals that apoptosis can proceed without Mcl-1 degradation, *J. Cell. Biol.* 180 (2008) 341–355.
- [8] Z. Zhang, T. Song, T. Zhang, G. Wu, J. Gao, L. An, G. Du, A novel BH3 mimetic S1 potently induces Bax/Bak-dependent apoptosis by targeting both Bcl-2 and Mcl-1, *Int. J. Cancer* 128 (2011) 1724–1735.
- [9] Z. Zhang, G. Wu, F. Xie, T. Song, X. Chang, 3-thiomorpholin-8-oxo-8H-ace-naphtha [1,2-b]pyrrole-9-carbonitrile (S1) based molecules as potent, dual inhibitors of B-cell lymphoma 2 (Bcl-2) and myeloid cell leukemia sequence 1 (Mcl-1): structure-based design and structure–activity relationship studies, *J. Med. Chem.* 4 (2011) 1101–1105.
- [10] P.J. Hajduk, J. Greer, A decade of fragment-based drug design: strategic advances and lessons learned, *Nat. Rev. Drug Discov.* 6 (2007) 211–219.
- [11] A.A. Alex, M.M. Flocco, Fragment-based drug discovery: what has it achieved so far? *Curr. Top. Med. Chem.* 7 (2007) 1544–1567.
- [12] M. Congreve, G. Chessari, D. Tisi, A.J. Woodhead, Recent developments in fragment-based drug discovery, *J. Med. Chem.* 51 (2008) 3661–3680.
- [13] G. Chessari, A.J. Woodhead, From fragment to clinical candidate – a historical perspective, *Drug Discov. Today* 14 (2009) 668–675.
- [14] M.N. Schulz, R.E. Hubbard, Recent progress in fragment-based lead discovery, *Curr. Opin. Pharmacol.* 9 (2009) 615–621.
- [15] C.W. Murray, M.G. Carr, O. Callaghan, G. Chessari, M. Congreve, S. Cowan, J.E. Coyle, R. Downham, E. Figueroa, M. Frederickson, B. Graham, R. McMennamin, Fragment-based drug discovery applied to Hsp90. Discovery of two lead series with high ligand efficiency, *J. Med. Chem.* 53 (2010) 5942–5955.
- [16] (a) D.A. Erlanson, R.S. McDowell, T. O'Brien, Fragment-based drug discovery, *J. Med. Chem.* 47 (2004) 3463–3482;
- (b) D.A. Erlanson, Fragment-based lead discovery: a chemical update, *Curr. Opin. Biotechnol.* 17 (2006) 643–652.
- [17] A.L. Hopkins, C.R. Groom, A. Alex, Ligand efficiency: a useful metric for lead selection, *Drug Discov. Today* 9 (2004) 430–431.
- [18] C. Abad-Zapatero, J.T. Metz, Ligand efficiency indices as guide-posts for drug discovery, *Drug Discov. Today* 10 (2005) 464–469.
- [19] (a) C.H. Reynolds, S.D. Bembenek, B.A. Tounge, The role of molecular size in ligand efficiency, *Bioorg. Med. Chem. Lett.* 17 (2007) 4258–4261;
- (b) S.D. Bembenek, B.A. Tounge, C.H. Reynolds, Ligand efficiency and fragment-based drug discovery, *Drug Discov. Today* 14 (2009) 278–283.
- [20] S. Schultes, C. de Graaf, E.E.J. Haaksma, I.J.P. de Esch, R. Leurs, O. Kraamer, Ligand efficiency as a guide in fragment hit selection and optimization, *Drug Discov. Today* 7 (2010) 157–161.
- [21] L. Hao, J. Zhou, Y. Sun, studies on the synthesis of gimeracil, *J. Shengyang Pharm. Univ.* 22 (2005) 420–421.
- [22] R. Church, R. Trust, J.D. Albright, D.W. Powell, New synthetic routes to 3-, 5-, and 6-aryl-2-chloropyridine, *J. Org. Chem.* 60 (1995) 3750–3758.
- [23] I. Stoll, R. Brodbeck, B. Neumann, H.G. Stammer, J. Mattay, Controlling the self assembly of arene functionalised 2-aminopyrimidines by arene-per-fluoroarene interaction and by silver(I) complex formation, *Cryst. Eng. Commu-n.* 11 (2009) 306–317.
- [24] L.C. Meurer, P.E. Finke, S.G. Mills, T.F. Walsh, Synthesis and SAR of 5,6-diarylpyridines as human CB1 inverse agonists, *Bioorg. Med. Chem. Lett.* 15 (2005) 645–651.
- [25] B.L. Duell, J.A. Bristo1, R.E. Weishaar, D.B. Evans, 1,2-dihydro-5-[4-(1H-imidazol-1-yl)phenyl]-6-methyl-2-oxo-3-pyridinecarbonitriles and related compounds synthesis and inotropic activity, *J. Med. Chem.* 30 (1987) 1023–1029.
- [26] D. Fattori, Molecular recognition: the fragment approach in lead generation, *Drug Discov. Today* 9 (2004) 229–238.
- [27] C. Yang, S. Wang, Analysis of flexibility and hotspots in Bcl-xL and Mcl-1 proteins for the design of selective small-molecule inhibitors, *Med. Chem. Lett.* (2012). doi:org/10.1021/ml200301w.
- [28] Moore V. Del Gaizo, K.D. Schlis, S.E. Sallan, S.A. Armstrong, A. Letai, Bcl-2 dependence and ABT-737 sensitivity in acute lymphoblastic leukemia, *Blood* 111 (2008) 2300–2309.
- [29] K.J. Aichberger, M. Mayerhofer, M.T. Krauth, H. Skvara, S. Florian, K. Sonneck, C. Akgul, S. Derdak, W.F. Pickl, et al., Identification of mcl-1 as a BCR-ABL-dependent target in chronic myeloid leukemia (CML): evidence for cooperative antileukemic effects of imatinib and mcl-1 antisense oligonucleotides, *Blood* 105 (2004) 3303–3311.
- [30] G. Wang, Z. Nikolovska-Coleska, C.Y. Yang, R. Wang, G. Tang, J. Guo, S. Shangary, S. Qiu, W. Gao, D. Yang, J. Meagher, J. Stuckey, K. Krajewski, S. Jiang, P.P. Roller, H.O. Aabaan, Y. Tomita, S. Wang, Structure-based design of potent small-molecule inhibitors of anti-apoptotic Bcl-2 proteins, *J. Med. Chem.* 49 (2006) 6139–6142.
- [31] Z. Nikolovska-Coleska, R. Wang, X. Fang, H. Pan, Y. Tomita, P. Li, P.P. Roller, K. Krajewski, N.G. Saito, J.A. Stuckey, S. Wang, Development and optimization of a binding assay for the XIAP BIR3 domain using fluorescence polarization, *Anal. Biochem.* 332 (2004) 261–273.